第34卷 第6期 焊 接 学 报 Vol. 34 No. 6
2013年6月 TRANSACTIONS OF THE CHINA WELDING INSTITUTION June 2013

搅拌摩擦焊待焊界面消失模型

王卫兵[1]， 佟建华[1]， 栾国红[1]， 董春林[1]， 聂绪胜[2]
(1. 北京航空制造工程研究所 中国搅拌摩擦焊中心，北京 100024;
2. 湖北三江航天科工集团红阳机械厂，孝感 432000)

摘 要: 提出了一种搅拌摩擦焊接过程中待焊界面消失并形成焊缝的二维模型，阐述了搅拌摩擦焊接过程中待焊界面在焊接热、焊接作用力及搅拌作用下形成焊缝的过程，并把焊缝划分成晶粒长大区、界面氧化区、待焊界面消失区、塑性金属流动区、S线等区域，同时描述了待焊界面冶金熔合后在搅拌摩擦焊缝内部的分布形态. 该模型对晶粒长大区、待焊界面消失区、S线3个特定区域进行了试验验证和说明. 结果表明，待焊界面在搅拌针后退侧的前方区域已经达到冶金熔合状态，并在搅拌针的搅拌作用下扭曲并进入焊缝形成S线特征.

关键词: 搅拌摩擦焊; 待焊界面消失区; 晶粒长大区
中图分类号: TG453.9 **文献标识码:** A **文章编号:** 0253-360X(2013)06-0037-04


王卫兵

0 序 言

搅拌摩擦焊(friction stir welding, FSW)自诞生至今已发展超过20年，在航空航天、轨道交通、电力电子等工业领域已经发展成为主要焊接工艺[1]. 但是搅拌摩擦焊焊缝的形成过程，没有形成一个明确的理论. 工艺参数的优化确定往往凭操作者的经验，还没有关于消除待焊界面的系统理论依据.

目前塑性金属材料的流动是搅拌摩擦焊焊缝成形机理的主要研究方向，诸多学者进行了大量的试验理论研究，Colligan[2]以小钢球作为示踪材料观察了塑性金属的流动规律，柯黎明等人[3]以铜片为标示材料研究了塑性金属流动，并提出了焊缝金属在水平面上的二维挤压模型. 王大勇等人[4]建立了塑性材料流动的三维模型，把流动区域划分为上、中和下3层. 正是塑性金属流动规律的揭示，搅拌头工具等焊接条件的优化有了理论依据，但是没有系统回答搅拌摩擦焊的待焊界面是如何消失的问题. 在此提出FSW待焊界面消失模型，并结合试验结果阐述FSW焊接过程中待焊界面是如何消失的，为工程中工艺参数的优化提供理论支持.

1 模型的提出

文中模型的研究对象为FSW尾孔附近且平行于焊缝上表面的水平纵截面，文中模型是基于二维空间的模型. 首先提出“待焊界面消失区”概念，待焊界面是指搅拌头前侧没有搅拌到的对接形式接头的对接面，随着FSW焊接过程的进行，待焊界面进入待焊界面消失区而形成FSW接头. 如图1所示，界面消失区位于FSW后退侧靠近搅拌针的区域，在该区域中，待焊界面受到焊接热、搅拌头的作用力及搅拌针的搅拌三重作用，焊接界面处发生冶金熔合形成连接，冶金熔合的待焊界面同时在搅拌针的搅拌作用下扭曲碎化成断续状，并随着塑性金属流动进入FSW焊缝中. 待界面消失区中的焊接热来源于两部分，分别为搅拌工具与焊接材料间的摩擦热以及焊接零件母材的高应变率大变形产生的变形热. 搅拌针的搅拌作用包含两方面作用，一方面是材料的转移，将塑化的焊接材料从前进侧转移到后退侧，另一方面是搅拌针上的螺纹、槽等结构对待焊界面的碎化作用. 搅拌头的作用力包括搅拌针的前进抗力、轴肩的顶锻力，还包括待焊界面消失区的内压力，该内压力的产生是因搅拌针对材料的转移作用造成的材料在后退侧的堆积. 待焊界面在上述热、搅拌、力三方面的综合作用下，形成冶金熔合而实现连接，并进入FSW的焊核中.

晶粒长大区，位于搅拌针的前侧且靠近待焊界面消失区，主要分布在靠近待焊界面的狭窄区域. FSW焊接过程中，焊接热量沿着待焊界面迅速传导，同时在搅拌头作用力的作用下，晶粒迅速长大，试验表明晶粒尺寸可长大到毫米级. 界面氧化区，

收稿日期: 2013-01-09
基金项目: 航空科学基金资助项目(2012ZE25007)

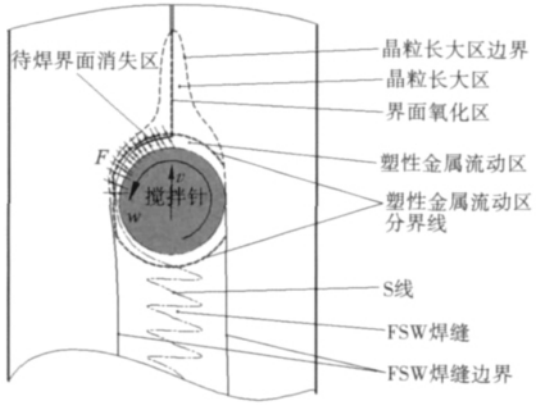

图1 FSW 待焊界面消失模型

Fig. 1 Model for disappearance of FSW pre-welding interface

位于晶粒长大区内，主要是指晶粒长大区中的两个待焊界面处，此区域的开敞性、热力条件和时间条件可以满足晶粒迅速长大，因而也满足待焊界面的氧化条件（虽然对接界面焊前机械打磨）. 塑性金属流动区，位于搅拌针周围的圆环区域. 因为搅拌针的高速旋转，搅拌针附近的焊接材料塑化，同时在搅拌针的驱动作用下，在靠近搅拌针很小的不规则圆环区域内，塑化焊接材料绕搅拌针发生不规则的塑性金属流动. S 线是指待焊界面经过晶粒长大区（包括界面氧化区），待焊界面消失区而绕过搅拌针进入 FSW 的焊核中，并呈周期性分布在 FSW 的焊核内部[图].

2 试验方法

为了验证模型的合理性，选用 4.5 mm 厚 6005 铝合金，焊接参数为焊接速度 1 400 mm/min，旋转频率 600 r/min. 搅拌头轴肩直径 13 mm，搅拌针的直径 4.3 mm，搅拌针的结构为右旋螺纹，焊接主轴旋转方向为逆时针. 试验研究对象根据文中模型所选，平行于焊缝上表面并距离焊缝上表面 1 mm. 通过对试验件选定区域的金相试验结果的分析，重点验证模型对晶粒长大区（A 区）、界面消失区（B 区）、S 线（C 区）3 个区域描述的合理性，具体位置如图 2 所示.

3 试验分析与结果

3.1 A 区试验结果分析

图 3 为 A 区（晶粒长大区）的金相试验结果，该区域的粗大晶粒分布在待焊界面的两侧. 待焊接界面处在焊接热的作用下，界面处晶界界面能较大，晶粒会优先发生合并长大，同时待焊接界面处还受到搅拌头的顶锻力和前进抗力两个方向的综合作用，此处变形极易达到临界变形量，再结晶后晶粒迅速长大到特别粗大的晶粒. 试验结果表明，A 区的晶粒长大到了毫米级，验证了晶粒长大区的存在性.

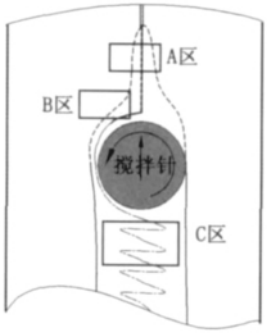

图2 试验取样示意图

Fig. 2 Schematic of specimen position

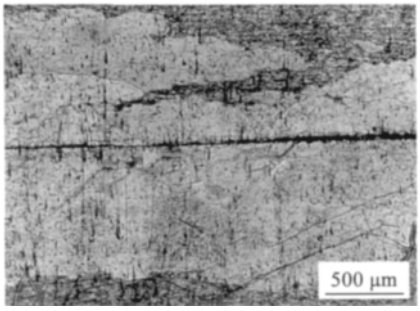

图3 A 区试验结果

Fig. 3 Result of zone A

3.2 B 区试验结果分析

图 4 为 B 区（界面消失区）的金相试验结果，在此区域内 FSW 待焊界面在焊接过程中产生的热、力（F）、搅拌的多重作用，最终此界面出现冶金熔合，而形成连接. 同时该区域的前一过程为晶粒长大区域，当晶粒长大区域向界面消失区转移的过程中，力和热的作用在熔合待焊界面的同时也碎化粗大的晶粒. 试验结果表明，界面消失区存在明显晶粒细化过程，同时 FSW 焊接界面处的晶粒尺寸表明该区域达到冶金熔合状态，即实现 FSW 连接.

3.3 C 区试验结果分析

图 5 为 C 区（S 线）的金相试验结果，该区域取自平行于工件上表面的水平方向内. 在扫描电镜下，S 线特征清晰可见，呈现断续的波浪周期分布，周期与“焊接速度/焊接旋转频率”呈周期性对应关

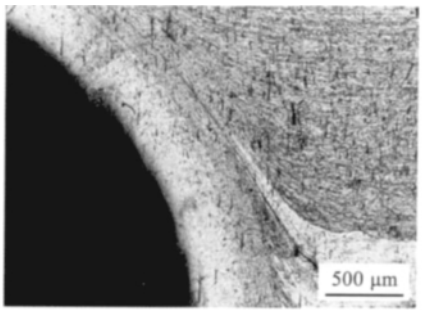

图 4　B 区金相试验结果

Fig. 4　Result of zone B

系. 在界面消失区,焊接界面处虽然达到冶金熔合,但是界面处具有特殊的热、力条件,组织结构和成分均有别于焊核其它区域. 同时在搅拌针螺纹、槽等结构的碎化作用下,S 线呈现断续现象.

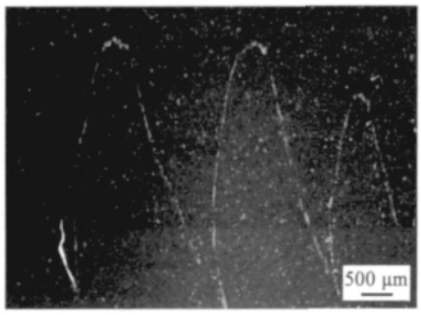

图 5　C 区试验结果

Fig. 5　Result of zone C

4　讨　　论

文中提出了一种搅拌摩擦焊的待焊界面消失模型,首次提出了界面消失区、晶粒长大区的概念. 较为系统地阐述了搅拌摩擦焊接过程中 FSW 连接的形成过程,同时借助对界面消失区、晶粒长大区、S 线区的试验验证,表明该模型具有一定的合理性. 在此利用待焊界面消失模型对 FSW 中的几个工程应用问题说明如下.

(1) 搅拌工具的轴线与焊缝的偏移关系,如图 6 所示,在实际 FSW 生产过程中,经常遇到搅拌针中心与焊缝的位置不重合的情况,如图 6a,c 两种情况. 根据待焊界面消失模型理论,图 6a 情况比图 6c 情况有利于焊缝的成形,因为图 6a 左偏时,待焊界面消失区更大,待焊界面处所承受的力和热的作用时间更长,有利于 FSW 焊缝的形成.

(2) 生产过程中当零件的对接间隙较大时,往

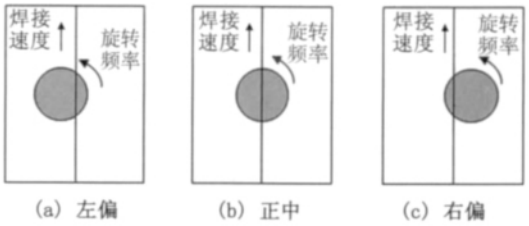

图 6　搅拌针与焊缝的位置关系

Fig. 6　Position relation between weld and pin

往选用较低的焊接速度及较大的焊接压入量以保证焊缝的质量. 根据界面消失模型理论,焊接旋转频率一定的情况下,焊接速度越慢,搅拌头旋转一周沿焊缝方向移动的距离越小,也就是界面消失区的材料越少(即界面消失区的宽度越小),待焊界面处热、力作用越显著,同时有利于搅拌针的搅拌作用,另外增大压入量进一步增加了待焊界面消失区的内压力,有利于待焊界面的冶金熔合. 当对接间隙过大时,待焊界面消失区难以形成稳定的热、力条件,同时对接间隙的存在使待焊界面消失区没有足够的内压力. 因而当对接间隙过大时,待焊界面处会出现孔洞缺陷,也就是 S 线上分布有大量的孔洞. 上述分析,也同样说明 S 线在特定的焊接状态下,不但组织特征有差异,还存在大量的微孔洞体积缺陷.

(3) 焊接过程中的氧化问题,根据待焊界面消失模型理论,存在一个晶粒长大区域,该区域的热、力学和时间条件可以使晶粒长大到毫米级,因而也可以使待焊对接界面氧化. 说明了焊缝中 S 线区域的氧的含量较其它焊核区域高. 同时也解释了虽然焊前对 FSW 零件进行严格的去氧化皮处理,但是 FSW 焊核中依然存在 S 线特征.

(4) 搅拌摩擦焊 S 线特征普遍存在于薄板对接接头中,而在厚板搅拌摩擦焊接头中不明显. 根据待焊界面消失模型理论,厚板焊接过程中,界面消失区的热、力条件更加充分. 另外厚板所用搅拌针的螺纹深度较大,在界面消失区对界面的碎化程度更大,也就是塑性金属流动更加充分. 塑性金属流动区的范围更大,待焊界面消失区与塑性金属流动区重合的区域更大,因而待焊界面被碎化的更加充分. 以上 3 方面因素导致厚板的 FSW 接头中 S 线特征不明显.

(5) 利用该模型还可以解释 Elangovan[6] 的方形搅拌针所获得接头硬度最高的试验结论. 如图 7 所示,搅拌针为方形时待焊界面消失区内的材料受到的塑性变形量更大,待焊界面消失区存在一条直线边界,当塑性材料向搅拌针后侧转移的过程中,方形

搅拌针的平面及棱边会驱动塑性材料流动产生更大的变形量,从而导致材料的晶粒更细化,所获得接头硬度更高.

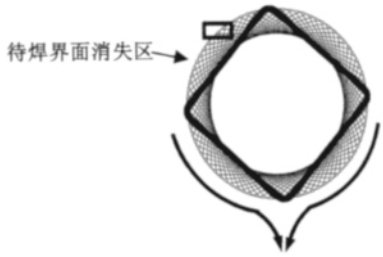

图7 方形搅拌针

Fig. 7 Square-shaped stirring pin

5 结 论

(1) 搅拌摩擦焊焊缝的形成过程中,待焊界面附近存在晶粒长大区域. 在焊接力的作用下,长大的晶粒碎化,同时界面处达到冶金熔合状态并实现连接,搅拌摩擦焊焊缝形成的区域位于搅拌针左前侧的待焊界面消失区.

(2) 搅拌针的前侧对接界面处在焊接热的作用下被氧化,氧化层在搅拌工具搅拌作用下随塑性金属进入焊缝,并呈S线特征分布在焊核内. 从侧面证明了S线特征区域的氧化物高于焊核其它部位的提法.

(3) 为了保证待焊界面消失区的内压力,应严格控制焊接位置对接间隙和焊接过程中的压入量. 当对接间隙过大时,可通过增大焊接压入量来保证焊缝的质量.

参考文献:

[1] 栾国红. 轻合金搅拌摩擦焊技术及新发展[J]. 航空制造技术, 2009, (9): 26-31.
Luan Guohong. Friction stir welding technology of light alloy and its new development[J]. Aeronautical Manufacturing Technology, 2009(9): 26-31.

[2] Colligan K. Material flow behavior during friction stir welding of aluminum[J]. Welding Journal, 1999, 78(7): 229s-237s.

[3] 柯黎明, 邢 丽. 搅拌摩擦焊接头形成过程的二维观察与分析[J]. 焊接学报, 2005, 26(3): 1-3.
Ke Liming, Xing Li. Two dimensional flow of plasticized materials in friction stir welded joints[J]. Transactions of the China Welding Institution, 2005, 26(3): 1-3.

[4] 王大勇, 冯吉才. 搅拌摩擦焊接三维流动模型[J]. 焊接学报, 2004, 25(4): 46-50.
Wang Dayong, Feng Jicai. Three dimensional flow modeling of friction stir welding[J]. Transactions of the China Welding Institution, 2004, 25(4): 46-50.

[5] 刘会杰, 张会杰, 黄永宪, 等. 搅拌摩擦焊缺陷的补焊方法[J]. 焊接学报, 2009, 30(1): 1-5.
Liu Huijie, Zhang Huijie, Huang Yongxian, *et al*. Study of repair welding technology of friction stir welding defects[J]. Transactions of the China Welding Institution, 2009, 30(1): 1-5.

[6] Elangovan K. Effect of tool pin profile and tool rotational speed on mechanical properties of friction stir welded AA6061 aluminum alloy[J]. Materials and Manufacturing Process, 2008, 23(3): 251-260.

作者简介: 王卫兵,男,1983年出生,硕士研究生,工程师. 主要从事搅拌摩擦焊工艺、装备及工程应用研究. 发表论文5篇. Email: 13811355411@163.com

changed to tearing through the welded seam when the crack propagated to the back side, and the tensile strength of the joint was 139 MPa. In contrast, the interface of the joints with Al-Cu-La filler exhibited dual layers, containing $TiAl_3$ and $Ti_2Al_{20}La$ phases. The fracture happened along the interface between $TiAl_3$ layer and Ti alloy substrate. The microcracks at the interface acted as the crack sources during the tensile test, and the fracture occurred in the interfacial layer with quasi-cleavage features. The tensile strength of joint with Al-Cu-La filler reached 270 MPa. The double compound layers formed due to the effect of La, which was the key to improve the joint strength.

Key words: Ti/Al dissimilar joint; arc fusion-brazing; interfacial reaction layer; facture behavior

Model for pre-welding interface disappearance of FSW

WANG Weibing[1], TONG Jianhua[1], LUAN Guohong[1], DONG Chunlin[1], NIE Xusheng[2] (1. FSW Center, BAMTRI China, Beijing 100024, China; 2. Hongyang Machinery Plant, China Sanjiang Aerospace Group, Xiaogan 432000, China). pp 37 – 40

Abstract: A 2D model for the disappearance of pre-welding interface and formation of FSW weld during friction stir welding (FSW) process was established. The forming process of friction stir weld from the pre-welding interface under the combined effects of welding heat, welding force and the stirring was described, and the friction stir weld can be divided into the grain growth zone, interface oxidizing zone, the pre-welding interface disappeared zone, plastic metal flow zone and "S" line zone. Meanwhile, the distribution of the pre-welding interface inside the weld was also identified in this paper. The model verified and explained the grain growth zone, "S" line and the pre-welding interface disappeared zone. The results showed that the pre-welding interface was in metallurgical fusion state in the front of retreating side, and it twisted into the weld shaping "S" line under the stirring of the tool pin.

Key words: friction stir welding; pre-welding interface disappeared zone; grain growth zone

Fatigue properties of Al-Mg-Mn-Zr-Er alloy and its laser welded joints

YANG Dongxia[1], LI Xiaoyan[1], GU Changshi[2], HE Dingyong[1], YAN Hailiang[1] (1. School of Materials Science and Engineering, Beijing University of Technology, Beijing 100124, China; 2. Shipbuilding Technology Research Institute, Shanghai 200032, China). pp 41 – 44

Abstract: Tensile and fatigue properties of Al-Mg-Mn-Zr-Er alloy and its laser welded joints were investigated, and the corresponded S-N curves and conditional fatigue limits were obtained. The microstructure and fatigue fracture were observed to explore the main causes of fatigue failure of Al-Mg-Mn-Zr-Er alloy laser welded joint. The results show that the microstructure of the joint was inhomogeneous. The base metal consisted of typical rolled structures, but the fusion zone mainly comprised small equiaxed grains with a size of 40 μm, and the heat-affected zone was recrystallized microstructure. The tensile strength of the welded joints was lower than that of base metal, and the joint strength coefficient was 0.73. The conditional fatigue limits of the welded joint was 68.5% of that of the base metal, and the main influence of fatigue performance were the microstructure inhomogeneity in the joint and the second phase inclusions in the weld.

Key words: Er-containing aluminum alloy; laser welding; fatigue life

Thickness effect on fracture toughness of A7N01P-T5 aluminum alloy

WANG Ping, LIU Xuesong, WANG Qiang, FANG Hongyuan (State Key Laboratory of Advanced Welding and Joining, Harbin Institute of Technology, Harbin 150001, China). pp 45 – 48

Abstract: Based on the present fracture toughness test methods for metallic materials, the fracture toughness K_C of A7N01P-T5 aluminum alloy was first tested according to the national standard GB4161-2007 and the corresponded analysis was also carried out. The new analytical formula of fracture toughness, which was related to the plate thickness, was proposed based on the energy theory and linear elastic mechanics. CTOD test was conducted to verify the accuracy of the new formula. The results show that the analytical formula could be used for various plate thicknesses, and also it could provide theoretical guidance for testing fracture toughness of other metallic materials. This work could not only save manpower and material resources, but significantly reduce the calculation cycle of remaining life of structures in structural integrity assessment of welded structures. Meanwhile, it also provides general methods and reference rules for obtaining the K_C of other metallic materials.

Key words: A7N01P-T5 aluminum alloy; fracture toughness; thickness effect

Composite-diffusion bonding of carbon fiber reinforced C_f/SiC composite and Ti alloy with (Ti-Zr-Cu-Ni) + W composite filler

CUI Bing, HUANG Jihua, CAI Chuang, CHEN Shuhai (School of Materials Science and Engineering, University of Science and Technology Beijing, Beijing 100083, China). pp 49 – 52

Abstract: Carbon fiber reinforced SiC (C_f/SiC) was successfully vacuum brazed to Ti alloy with (Ti-Zr-Cu-Ni) + W composite filler at 930 ℃ for 5 min. The interface microstructure was investigated with scanning electron microscope (SEM), energy dispersive spectrometer (EDS) and X-ray diffraction (XRD). The mechanical properties of the brazed joints were measured by mechanical testing machine. The results show that Ti and Zr in the interlayer can react with the C_f/SiC composite, and the brazed seams mainly consist of Ti_3SiC_2, Ti_5Si_3, and some TiC(ZrC) reaction products. The mutual diffusion between Ti from the Ti alloy substrate and Cu and Ni from the interface formed the diffusion-reaction layer between the interlayer and Ti alloy substrate. After heat treating the brazed joint at 900 ℃ for 60 min, the interlayer microstructure became homogenization and the diffusion layer on TC4 alloy side thickened, and the shear strength of the joint reached 99 MPa, increased 52% comparing with that (65 MPa) before heat treatment.

Key words: C_f/SiC composite; Ti alloy; composite-diffusion bonding

Harden quenching tendency and cold cracking susceptibility of Q890 steel during welding

ZHANG Yuanjie[1,2], PENG Yun[1,2], MA Chengyong[2], PENG Xinna[2], TIAN Zhiling[2], LU Jiansheng[1] (1. School of Materials Science and Engineering, Kunming University of Science and Technology, Kunming 650093, China; 2. China Iron and Steel Research Institute Group, Beijing 100081, China). pp 53 – 56

Abstract: The harden quenching tendency and cold cracking susceptibility of Q890 steel was investigated by welding thermal simulation, maximum hardness test and calculation with empirical formula. The results show that the empirical formula